CNT-based gas ionizers with integrated MEMS gate for portable mass spectrometry applications

CNT-BASED GAS IONIZERS WITH INTEGRATED MEMS GATE FOR PORTABLE MASS SPECTROMETRY APPLICATIONS

L.F. Velásquez-García[1], B. Gassend[2], and A.I. Akinwande[1,3]*

[1]Microsystems Technology Laboratories, Massachusetts Institute of Technology, Cambridge, MA, USA
[2]Exponent Inc., Menlo Park, CA, USA
[3]Electrical Engineering and Computer Science, Massachusetts Institute of Technology, Cambridge, MA, USA

ABSTRACT

We report the fabrication and experimental characterization of a novel low-cost carbon nanotube (CNT)-based electron impact ionizer (EII) with integrated gate for portable mass spectrometry applications. The device achieves low-voltage ionization using sparse forests of plasma-enhanced chemical vapor deposited (PECVD) CNTs field emitter tips, and a proximal gate with open apertures to facilitate electron transmission. The gate is integrated using a deep reactive ion etched (DRIE) spring-based high-voltage MEMS packaging technology. The device also includes a high aspect-ratio silicon structure (µfoam) that facilitates sparse CNT growth and limits the electron current per emitter. The devices were tested as field emitters in high vacuum (10^{-8} Torr). Electron emission starts at a gate voltage of 110 V, and reaches a current of 9 uA at 250 V (2.25 mW) with more than 55% of the electrons transmitted through the gate apertures. The devices were also tested as electron impact ionizers using Argon. The experimental data demonstrates that the CNT-EIIs can operate at mtorr-level pressures while delivering 60 nA of ion current at 250 V with about 1% ionization efficiency.

KEYWORDS

Carbon nanotubes (CNTs), DRIE, gas ionizer, electron impact ionization, field emission, portable mass spectrometry, 3D MEMS packaging.

INTRODUCTION

MEMS-based analytical instrumentation has been an active area of research for more than a decade. In particular, some research efforts have focused on the development of rugged gas chromatography and mass spectrometry (GC/MS) systems that are smaller, lighter, cheaper, faster, and more power efficient [1], [2]. The power consumption, size, and weight of these systems are driven by the pumping requirements. Therefore, the relaxation of the pressure level at which the system components can operate would enable its portability. Portable GC/MS systems, either as individual units or as part of massive networks, can be used in a wide range of applications including in-situ geological survey, law enforcement, environmental monitoring, and space exploration [3]–[5].

One of the core components of an MS system is the ionizer. In electron impact ionization, a stream of electrons is used to ionize neutral gas molecules by collision. The ratio between the ion current $I_I(E)$ to the electron the current $I_E(E)$ is

$$\frac{I_I(E)}{I_E(E)} = \frac{P}{K_b \cdot T} L \cdot \sigma_{total}(E) \qquad (1)$$

where E is the energy of the electrons, P is the gas pressure, K_b is Boltzmann's constant, T is the gas temperature, L is the collision path length (i.e., the distance between the electron source and the ion collector), and $\sigma_{total}(E)$ is the total ionization cross section. State-of-the-art EIIs for MS systems accomplish ionization using a thermionic electron source. Thermionic-based EIIs are power hungry (>1W), can only operate at low pressure (<10^{-5} torr) due to back-ion bombardment reliability, and have low ionization efficiency [6], [7]. Therefore, thermionic-based EIIs are not suitable for portable mass spectrometry.

A low-power approach to implement EIIs for portable MS systems involves the use a cold cathode. Electrons are field emitted from the surface of metals and semiconductors when the potential barrier that holds electrons within the material (workfunction) is deformed by the application of a high electrostatic field [8]. High surface electrostatic fields are typically obtained by the application of a voltage to a high aspect-ratio structure with nanometer-scaled tip radius. Field emission is described by the Fowler-Nordheim (FN) model, which predicts that the electron current $I_E(V_G)$ from a tip biased at a voltage V_G has an exponential dependence with respect to the field factor β [8]:

$$I_E(V_G) \propto V_G^2 \cdot \exp\left(\frac{-0.95 \cdot B \cdot \phi^{1.5}}{\beta \cdot V_G}\right) \qquad (2)$$

where $B = 6.87\times10^7$ and ϕ is the workfunction of the emitter tip. The inverse of the field factor has dimensions of length. The field factor relates the electric field at the tip surface to the applied gate voltage and it is to first order equal to the inverse of the emitter tip radius r.

DEVICE STRUCTURE AND DESIGN

Our NEMS/MEMS CNT-EII (Fig. 1) is composed of two parts which are 1) a main body and 2) a gate. The main body (Fig. 2) is a two-wafer stack that includes sparse arrays of plasma enhanced chemical vapor deposited (PECVD) CNTs, a high aspect-ratio silicon structure (μfoam), and a system of DRIE patterned springs to assemble the gate to the main body. The gate is a 1-cm wide disk-shaped component with a perforated grid that includes a set of notches that are used to lock-in the gate (Fig. 3, left). The μfoam structure and the gate grid do not line up (Fig. 3, right) because the gate is used as a shadow mask during the deposition of the CNT catalyst.

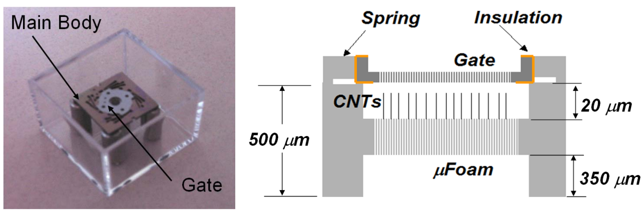

Figure 1: An assembled CNT-based gated electron impact ionizer (left), and cross-section of the device (right).

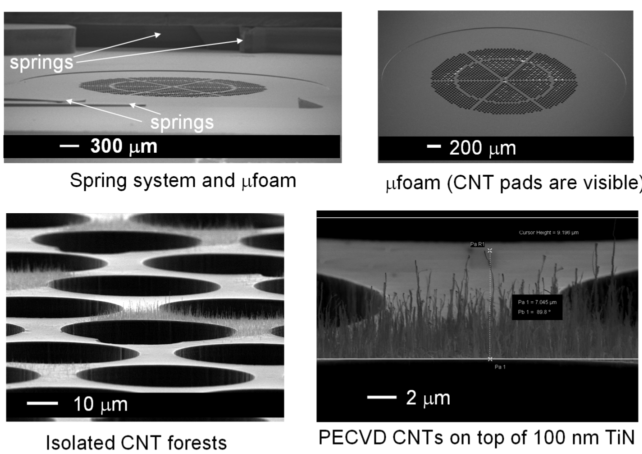

Figure 2: SEMs of the CNT-EII main body: spring assembly system (top left), μfoam (top right), sparsely grown CNTs (bottom left), and detail of the PECVD CNTs (bottom right).

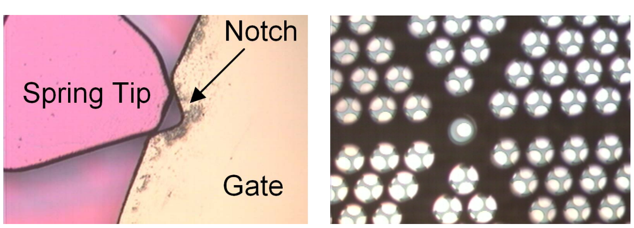

Figure 3: A DRIE-patterned assembly spring locked into a gate notch (left), and top view of the μfoam through an assembled gate using backside light (right).

Our CNT-EII includes a set of features to achieve low-voltage ionization, high-pressure operation, and device reliability. First, our device uses PECVD CNTs as field enhancers. CNTs are resilient high aspect-ratio graphitic structures with nano-scaled tip diameters ideal for field emission applications, particularly at high pressure. We had previously shown that sparse clusters of PECVD CNTs can be grown without high-cost/low-throughput methods such as e-beam lithography by depositing the CNT catalyst (Ni) on top of the μfoam [9]. Second, our ionizer uses a MEMS gate that effectively hovers a few microns above the PECVD CNT tips, resulting in low electron emission start-up voltage. The gate is integrated to the rest of the ionizer using a high-voltage MEMS packaging technology [10] that has micron-level assembly precision and micron repeatability [11]. The re-assembly precision makes it possible to use the gate as shadow mask to define the catalyst pads, grow the PECVD CNTs without the gate (this way the plasma sheath is not trapped by the gate, and the electrical insulation of the gate is not deteriorated due to exposure to the CNT plasma growth), and then to re-assemble the gate to obtain a functional device. The good re-assembly alignment precision between the gate and the CNT growth is reflected in the level of the gate interception current, which is more than an order of magnitude smaller than the gate interception using a similar emitting substrate with a non-aligned grid [9]. Finally, the data shows that our ionizer is current-limited, presumably because of velocity saturation of electrons within the μfoam, resulting in more uniform current emission [12], [13]. Un-ballasted field emitter arrays don't work uniformly because of the broad tip diameter size distribution and the strong dependence of the current emission on the emitter tip diameter as shown by Eq. (2).

In addition, the design of the ionizer intends to simplify the overall MS system integration by including a structure (i.e., the μfoam) that can serve as interface between the interior and the exterior of the MS. The μfoam acts as a perforated screen that feeds the external gas into the MS, at a rate controlled by the viscosity and the compressibility of the gas [14].

DEVICE FABRICATION

Two silicon wafers are required to fabricate the ionizer. The two wafers are used to fabricate the main body, while portions of one of the wafers are used to fabricate the MEMS gate. The main fabrication technologies used in the process flow are contact photolithography, fusion bonding, and DRIE. The PECVD CNTs are sparsely grown using a combination of selective growth [9] and shadow masking, using the PECVD CNT growth process described by Teo et al [15].

The ionizer gate is integrated using a high-voltage MEMS packaging technology based on DRIE-patterned mesoscaled deflection springs [10]. The gate is reversibly assembled with micron-level precision and micron repeatability, and it can also withstand large inertial forces without detaching [11]. This assembly technology makes it possible to define the CNT catalyst and grow the CNTs without affecting the electrical insulation of the device. Further details are given elsewhere [16].

EXPERIMENTAL CHARACTERIZATION

The CNT-EIIS were tested as field emitters and as electron impact ionizers. In both cases the gate was biased positive with respect to the main body, and there was an external ball collector biased at 1100V with respect to the main body of the CNT-EII.

The CNT-EIIs were tested as field emitters in high vacuum (10^{-8} Torr). The data shows that electron emission above the noise floor (10^{-11} A) starts at a gate voltage of 110 V, with an emitted electron current of 9 uA at 250 V (Fig. 4). More than 55% current transmission through the gate was measured. The percentage of current transmitted through the gate is more than an order of magnitude larger than the percentage of current transmitted we previously reported using a µfoam structure with a non-aligned grid [9]. We speculate that a larger current transmission could be obtained if the gate were able to apply a more symmetric electric field around the CNT tips. This is currently not possible due to fabrication constraints (the aperture of the gate grid would need to be of the order of the CNT-to-gate separation) and alignment limitations of the spring assembly. The emitted current is visibly smaller than the mA-level electron current we previously reported from the µfoam structure [9]. However, unlike in our previous report, the electron current coming out of the µfoam is clearly limited, as evidenced by the FN plot (Fig. 5). The current limitation effect seems to be related to the high aspect-ratio of the µfoam structure, and the high resistivity (> 50 Ω.cm) of the silicon substrate used to create it. The µfoam acts as an ungated field-effect transistor (FET) that limits the current due to velocity saturation of electrons in silicon [12], [13]. The linear part of the FN plot predicts a field factor β = 3.3×10^5/cm. Using ϕ = 4.8 eV, and assuming $\beta \sim r^{-1}$, it is estimated a CNT tip diameter equal to 61 nm, in good agreement with the 67 nm value from SEMs.

The devices were also tested as EIIs using Argon (Fig. 6). The device produces ion currents larger than the noise floor ($\sim 5\times10^{-12}$ A) at a gate voltage of 125 V and an acceleration voltage of 300 V. At a gate voltage of 250 V, and ion current of 60 nA was measured while operating at 1 mtorr. As shown in Fig. 7, the ion current scales linearly with the background pressure, as expected from Eq. (1). In addition, using the values $\sigma_{total} \sim 3\times10^{-16}$ cm^2, K_b = 1.38×10^{-23} J/K, T = 300 K, and $L \sim 3$ cm, an intercept equal to -1.52 is obtained vs. -1.31 from the linear fit of the data. Based on the field emission and electron impact ionization data, about 1% ionization efficiency is estimated when de ionizer operates at 1 mtorr. The ionization efficiency is defined as the number of ions per electron, i.e., the ratio between the ion current and electron current.

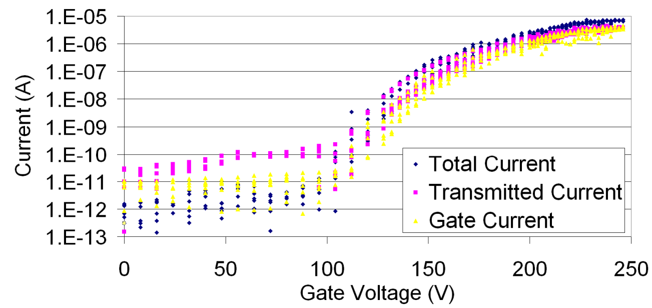

Figure 4: I-V characteristics, field emission.

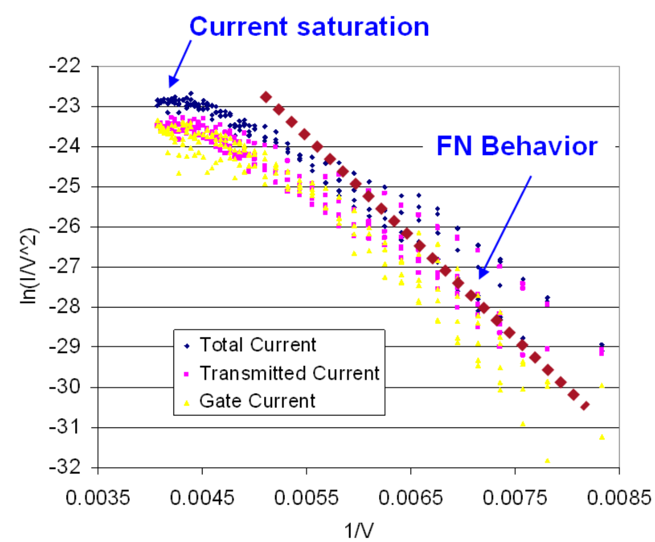

Figure 5: FN plot of I-V characteristics, field emission. The FN plot becomes flat for large enough (>220 V) bias voltages.

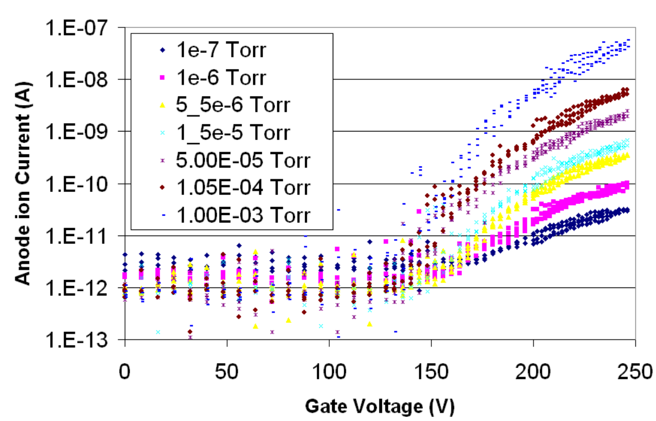

Figure 6: I-V characteristics, electron impact ionization.

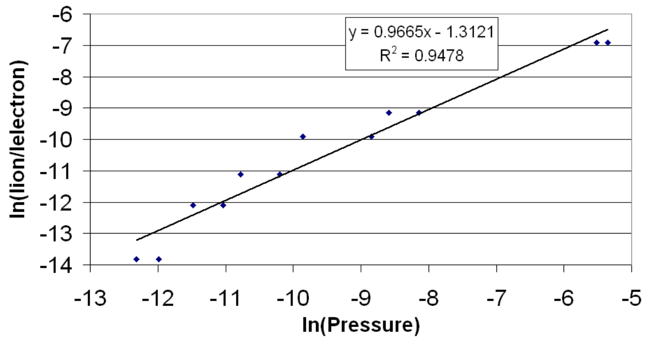

Figure 7: Ratio of ion current to electron current vs. pressure.

Our ionizer compares favorably with respect to the work reported by other researchers. For example, the electron current level and operational voltage is substantially larger than the performance of nanostructured boron nitride cathodes reported by Liu et al [17]. Also, the ionization efficiency is comparable to the ionization efficiency reported by Chen et al at a slightly higher pressure [18]. However, our ionizer should have higher ionization efficiency if operated at higher pressures. In addition, our ionizer has an estimated field factor in the linear part of the FN plot that is 50% larger than the corresponding values reported by Manohara et al [19], which should be related to the shadowing effect that their CNTs suffer due to their proximity within the same fiber.

REFERENCES

[1] S. C. Terry et al, "A gas chromatographic air analyzer fabricated on a silicon wafer," *in Proceedings IEEE Trans. Electron Devices*, vol. ED-26, no. 12, pp. 1880–1886, Dec. 1979.

[2] B. Ghodsian et al, "Gas detector with lowcost micromachined field ionization tips", *IEEE Electron Device Lett.,* vol. 19, no. 7, pp. 241–243, Jul. 1998.

[3] R. R. Reston and E. S. Kolesar, "Silicon-micromachined gas chromatography system used to separate and detect ammonia and nitrogen dioxide—Part I: Design, fabrication, and integration of the gas chromatography system," *J. Microelectromech. Syst.*, vol. 3, no. 4, pp. 134–146, Dec. 1994.

[4] R. R. Reston and E. S. Kolesar, "Miniature gas chromatography system realized using conventional VLSI fabrication techniques applied to quantifying toxic environmental pollutants," *in Proceedings IEEE NAECON,* May 1994, vol. 1, pp. 327–333.

[5] W. C. Wang, "Micromechanical devices at JPL for space exploration," *in Proceedings IEEE Aerosp. Conf.,* 1998, vol. 1, pp. 461–470.

[6] K. T. Tompson, "Theory of Ionization by Cumulative Action of Successive Impacts by Electrons and by Quanta of Resonance Radiation", *Phys. Rev.,* vol 20, pp. 283-299, 1922.

[7] E. de Hoffmann and V. Stroobant, *Mass Spectrometry: Principles and Applications*, John Wiley & Sons, West Sussex, England, 2002.

[8] R. Gomer, *Field Emission and Field Ionization*, American Institute of Physics, New York, 1961.

[9] L. F. Velásquez-García and A. I. Akinwande, "A PECVD CNT-based open architecture field ionizer for portable mass spectrometry", *in Proceedings IEEE MEMS 2008,* 13-17 Jan. 2008, pp. 742 – 745.

[10] L. F. Velásquez-García et al, "Precision Hand Assembly of MEMS Subsystems Using DRIE-Patterned Deflection Spring Structures: An Example of an Out-of-Plane Substrate Assembly", *J. Microelectromech. Syst.,* Vol. 16, No. 3, pp. 598–612, Jun. 2007.

[11] B. Gassend et al, "Precision In-Plane Hand Assembly of Bulk-Microfabricated Components for High-Voltage MEMS Arrays Applications", accepted for publication, *J. Microelectromech. Syst.,* DOI: 10.1109/JMEMS.2008.2011115

[12] H. Takemura et al, "A novel vertical current limiter fabricated with a deep trench forming technology for highly reliable field emitter arrays", *in Proceedings IEEE IEDM*, pp. 709-712, 1997.

[13] L.F. Velásquez-García, et al, "Uniform High Current Field Emission of Electrons from Si and CNF FEAs Individually Controlled by Si Pillar Ungated FETs", *in Proceedings IEEE IEDM*, Washington DC, pp. 599 – 602, 2007.

[14] P. H. Thompson, *Compressible-Fluid Dynamics*, Third Edition, McGraw-Hill, 1988.

[15] K.B.K. Teo et al, "Plasma enhanced chemical vapour deposition carbon nanotubes/nanofibers – how uniform do they grow?" *Nanotechnology* vol. 14, pp 204 – 211, 2003.

[16] L. F. Velásquez-García et al, "CNT-Based Field Emission Electron Impact Ionizers with MEMS Integrated Gate for Portable Gas Analyzers", in preparation.

[17] T. M. Liu et al, "Use of Boron Nitride for Field Effect Electron Emission", *AIAA/ASME/ASEE JPC*, Cincinnati OH, AIAA 2007-5253, 2007.

[18] L-Y. Chen et al, "A Micro Ionizer for Portable Mass Spectrometers using Double-gated Isolated Vertically Aligned Carbon Nanofiber Arrays", *in Proceedings IEEE IEDM*, Washington DC, pp. 843 – 846, 2007.

[19] H. M. Manohara et al, "Application Specific Electrode-integrated Nanotube Cathodes (ASINCs) for Miniature Analytical Instruments for Space Exploration", *in Proceedings of the SPIE*, Vol 6959, pp. 695906 – 695906-6, 2008.

CONTACT

* L.F. Velásquez-García, tel: +1-617-253-0730; lfvelasq@mit.edu